Study of Monthly Variation of Precipitable Water Vapor, Sensor Temperature, Dew Point Temperature, Rainfall and Relative Humidity using AERONET's CIMEL Sunphotometer in Lumbini, Nepal for May 2017 to May 2018

Balaram Khadka[1,2], Ankit Kumar Karn[1], Shubham Kumar Chaurasia[2], Sushil Kumar Bista[1], P C Thakuri[1]

[1]Department of Physics, St. Xavier's College, Maitighar, Kathmandu, Nepal
[2]Department of Physics, Trinity International College, Dillibazar, Kathmandu, Nepal

Abstract - **Precipitable Water Vapor (PWV) is one of the important parameters in the hydrologic cycle, energy exchange between the biosphere and the atmosphere. It plays a great role in modeling the flow of energy at the ground level which leads to climatic change. Thus, the estimation of PWV has great importance in studies of climatic change. Lumbini, Nepal is the site for collecting PWV data. In this research we have processed and analyzed PWV, sensor temperature and relative humidity obtained from CIMEL to get monthly and seasonal variation for May 2017 to May 2018. We have also studied possible correlation between sensor temperature, rainfall, dewpoint temperature and relative humidity with PWV. Maximum and minimum correlation between PWV and dew point temperature is 0.87081 and 0.00509 in September and May respectively. We found negative correlation between PWV and dewpoint temperature in the month of June, August and October. Maximum and minimum correlation between PWV and sensor temperature is 0.77957 and 0.25124 in the month of November and May respectively. We found negative correlation in the months of June and August. Maximum and minimum correlation of PWV and RH^2/T is 0.74719 and 0.17389 in the month of August and June. We found negative correlation in the month of May, September, October, November and December.**

***Keywords* - Precipitable Water Vapor, PWV, Sunphotometer**

I. INTRODUCTION

Water vapor plays a crucial role in climate change, hydrological processes as it is formed by evapotranspiration from the surface into the atmosphere, can condense into clouds and may return back to the surface in the form of precipitations. The feature of water molecules to warm the atmosphere by absorbing and reemitting infrared radiation makes water vapor an important component of green house gas and its affect on global warming is of interest. Precipitable water vapor (PWV) is the amount of liquid water that would be obtained if all the vapor in the atmosphere within the vertical column were compressed to the point of condensation. PWV is an indicator of water vapor quantity in the atmosphere. Therefore, having a precise measure of PWV can improve the monitoring/evaluation of climate and agricultural meteorology because it shows the location and movement of moisture. Latent heat of vaporization, which is released whenever atmospheric PWV condenses, is an important aspect of atmospheric energy budget that drives the movement of weather systems across the globe. We calculate these using measurements from weather balloons, from satellite data, or from weather and climate models. Source will be described in section II, methodology in section III, result in section IV and conclusion in section V.

II. EXPERIMENTAL SITE, DATA SOURCES, AND METHODS

As an important contribution to SusKat measurement campaign in Nepal, NASA's Aerosol Robotic Network (AERONET, http://aeronet.gsfc.nasa.gov/) project deployed CIMEL sun/sky radiometer in various locations such as Lumbini, Kathmandu, Bidur, Hetauda, and Jomsom. Among these locations, we selected Lumbini, Nepal (27.6792° N, 83.5070° E, 150 m elevation) as our experimental site, which lies on the southern side of the Nepal-Terai region. Lumbini, a pilgrimage site, has historical significance as the birthplace of Siddhartha Gautama, the propounder of Buddhism. It is the buffer region between the mountainous Himalayas and Indo-Gangetic plain and makes it a perfect site for the study of precipitable water vapor. It was declared as the World Heritage Site by UNESCO in 1997. The

study region has 251 cloudless days implying that 58.9 percent of days (including partly cloudy days) allows Sun photometer measurements.

The CIMEL sun photometer is set up in the premises of Lumbini International Research Institute (LIRI) in the 'Lumbini Master Plan Area.' It is covered with forest and Buddhist monasteries, lying in an agricultural-residential setting. The sun photometer records PWV data of Lumbini, and these data are provided by the website 'https://aeronet.gsfc.nasa.gov/.' Data from the AERONET are available in three levels - Level 1.0 (unscreened), Level 1.5 (cloud screened) and Level 2.0 (quality-assured data). In this study, we have used the Level 2.0 data, collected between May 2017 and May 2018. Good quality level 2.0 data was available for most of the seasons and is used in this study. Microsoft Excel software is used for data preparation while the origin software is used for plotting, curve fitting and other analysis. The statistical tools used for the data analysis are Pearson's correlation(R) and Root Mean Square Error whose calculation method is mentioned in methodology. The more the value of RMSE approaches to zero, the more model obtained is used as a predictor.
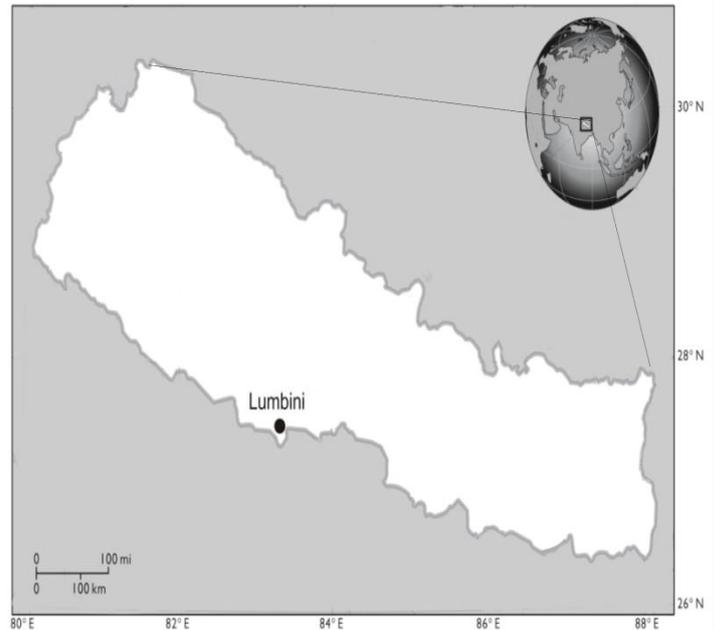

Fig.1. Map showing Lumbini, Nepal with photos of sampling tower at LIRI and CIMEL Sunphotometer.

III. METHODOLOGY

A) Derivation of precipitable water vapour from cimel observations

CIMEL sun photometer has been utilized in the AERONET network as an instrument to obtain direct sky and its radiance measurements at different wavelengths. This can be done using interference filters centered at 340, 380, 440, 670, 870, and 1020 nm to measure aerosol columnar properties. An additional filter is centered at 940 nm to retrieve precipitable water vapor (PWV). The full width at half maximum (FWHM) of the transmission bands of each of these filters is between 2 and 10 nm.

Table I
Showing basic principle of CIMEL Sunphotometer

Technique	Measurement principle	Estimated uncertainty	Data source
Sun photometry	Solar direct irradiance at 940nm absorption band.	±10% [e.g., Smirnov et al., 2004]	AERONET

Water vapor has the special property of absorbing and then re-emitting infrared radiation. The sun-photometer method relies on the interaction of the solar electromagnetic energy with the atmospheric constituents before the energy reaches the earth surface. This interaction leads to scattering and absorption from which the amount of atmospheric water could be deduced. Particularly, in the near infrared spectrum, around 940 nm, there is a strong wavelength-dependent absorption by water vapor and the response of the instrument. Microwave radio-meters [Westwater et al., 2006; Liljegren et al., 1999] (available at http://www.arm.gov/publications/proceedings/conf09/extended_abs/liljegren3_jc.pdf) use the interaction0 of an emitted microwave signal with the atmosphere to retrieve the water vapor, while infrared radiometers rely on measuring the thermal longwave radiation emitted by the atmosphere. Sun photometry has special property to deal with attenuation of radiation through the atmosphere and uses Beer Bouger Lambert law.

V (940 nm) to light in this spectral region is given by:

$$V(940\ nm) = V_0(940\ nm)d^{-2}\exp(-m_r\partial_{atm}(940\ nm))T_w(940\ nm)$$

where V_0 (940 nm) is the instrument calibration constant (signal that the instrument would measure if it were placed outside of the atmosphere), d is the Earth-Sun distance (in astronomical units) at the time of observation, m_r is the relative optical air mass, ∂_{atm}(940 nm) is the total atmospheric optical depth (excluding absorption by water vapor) and T_w(940 nm) is the water vapor transmittance around the 940 nm absorption bands. For the computation of ∂_{atm}(940 nm), the optical depths at 940nm due to molecular scattering, gas absorption (mainly very weak absorption bands of O_3 and NO_2), and aerosol (aerosol optical depth (AOD)) are computed following AERONET procedures [Holben et al., 1998]. The computation of V_0 (940 nm) and ∂_{atm} (940 nm) is done following AERONET procedures (Holben et al., 1998). For a straightforward retrieval of PWV, AERONET uses a simplified expression of T_w (940 nm) given by (Reagan et al., 1987; Bruegge et al., 1992)

$$T_w(940\ nm) = \exp(-a(m_w PWV)^b$$

Where m_w is the relative optical water vapor-air mass and a and b are coefficients that depend on the wavelength position, width, and shape of the sun-photometer filter function, and the atmospheric condition. Each AERONET instrument has its own unique set of ʻaʼ and ʻbʼ values depending on the filter configuration. These coefficients are considered fixed until the filter is changed.

The error associated to this technique depends on the error of the calibration constant V_0 and on the modeling of the water vapor transmittance (the contribution of Rayleigh scattering and aerosols is generally much lower). According to AERONET [Holben et al., 1998; Smirnov et al., 2004; Bokoye et al., 2007], the PWV retrieved for this technique is accurate to about 10%. However, the modeling of the 940 nm water vapor band is not straightforward because of the contribution of the continuum water vapor absorption [Cachorro et al., 1998; Ingold et al., 2000]

B) Calculation of Pearson's R AND root mean square error (RMSE)

PEARSON'S (R)

Pearson's R is the standard metric to measure the extent to which two variables are linearly related and fluctuates from -1 to +1 where -1 refers that there exists negative correlation while +1 refers there exists positive correlation.

It is defined as the ratio of the covariance of two variables representing a set of numerical data, normalised to the square root of their variances, i.e.:

$$r = \frac{C_{xy}}{\sqrt{C_{xx}C_{yy}}} = \frac{C_{xy}}{\sigma_x \sigma_y} \qquad (1)$$

or, in more detail, for a set of N two-dimensional data points [x1, x2, . . . , xN] and [y1, y2, . . . , yN], we have:

$$\bar{x} = \frac{1}{N}\sum_i x_i \qquad (2)$$

$$\bar{y} = \frac{1}{N}\sum_i y_i \qquad (3)$$

$$C_{xy} = \frac{1}{N-1}\sum_i (x_i - \bar{x})(y_i - \bar{y}) \qquad (4)$$

$$C_{xx} = \sigma_x^2 = \frac{1}{N-1}\sum_i (x_i - \bar{x})^2 \qquad (5)$$

$$C_{yy} = \sigma_y^2 = \frac{1}{N-1}\sum_i (y_i - \bar{y})^2 \qquad (6)$$

DEW POINT TEMPERATURE

The dew point is the temperature at which the water vapor contained in a volume of air at a given atmospheric pressure reaches saturation and condenses to form dew. A simplified approximation used to calculate the dew point (Td) starting from the actual air temperature (T) and relative humidity (RH), is the Magnus formula:

$$T_d = \frac{b\left[\ln\left(\frac{RH}{100}\right) + \frac{a.T}{b+T}\right]}{a - \ln\left(\frac{RH}{100}\right) - \frac{a.T}{b+T}} \qquad (7)$$

Where,
t = dew point temperature in ºC
RH = measured relative humidity in %
T = measured temperature in ºC
a =approximately 17.271
b =approximately 237.7

CALCULATION OF RMSE (ROOT MEAN SQUARE ERROR)

RMSE has been used as a standard metric to measure model performance in climate research. It is the square root of the mean squared error. It measures the differences between values predicted by a

hypothetical model and the observed values. In other words, it measures the quality of the fit between the actual data and the predicted model. *RMSE* is one of the most frequently used measures of the goodness of fit of generalized regression models.
Where

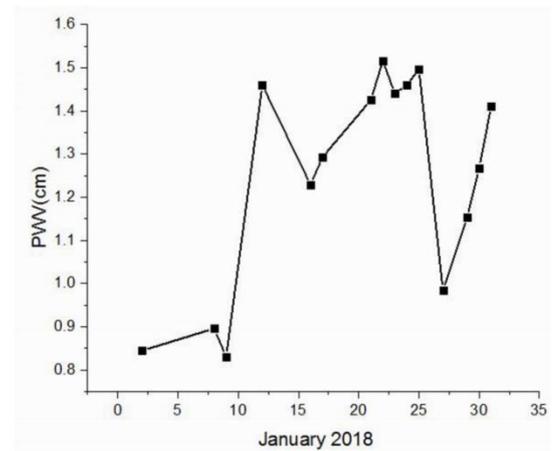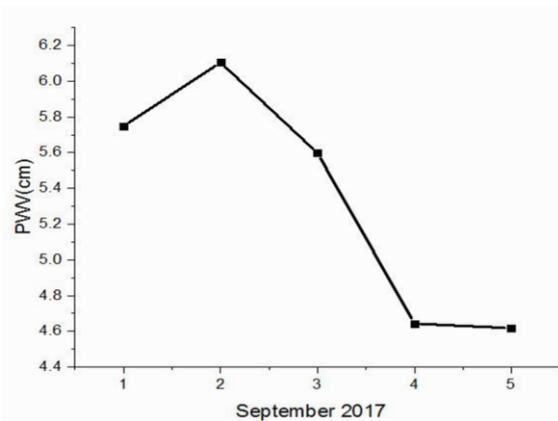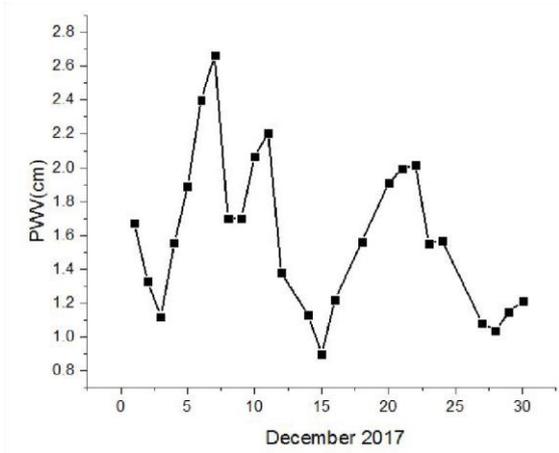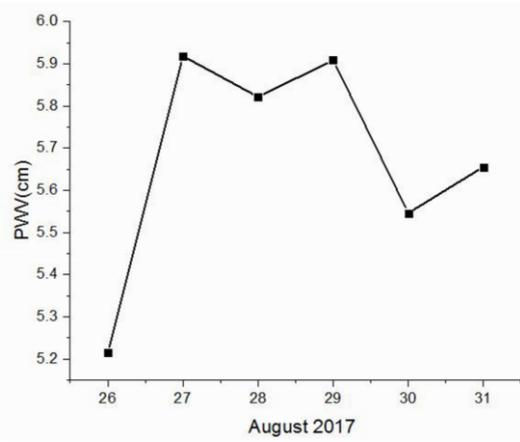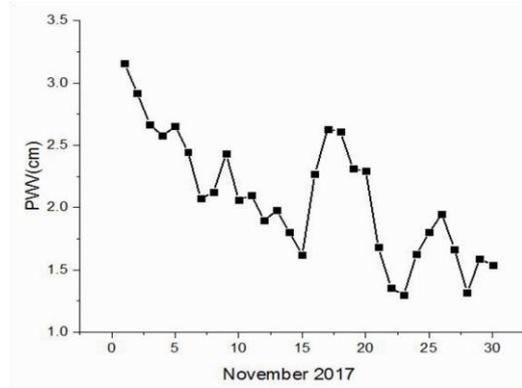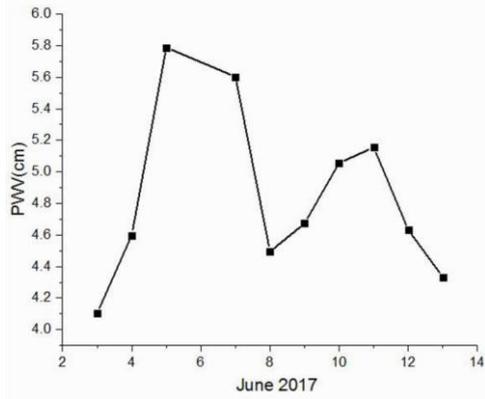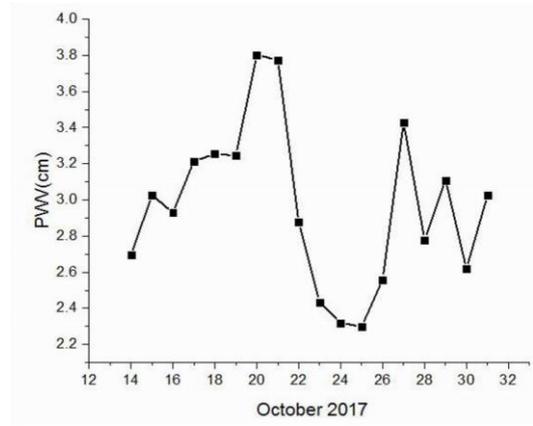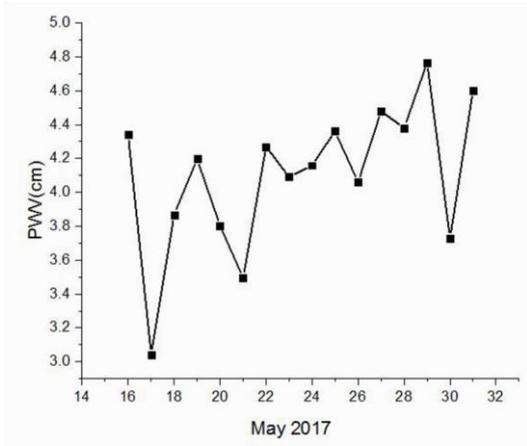$$RMSE = \frac{1}{n}\sum_{i=1}^{n}(y_{ie} - y_{im)}^2$$

Where, n is the number of data points; y_{ie} is the raw data value and y_{im} is the value obtained from the m empirical model. A value of RMSE closer to 0 indicates that the empirical model/equation has a smaller random error component.

IV. RESULT AND DISCUSSION

A) Monthly trend in PWV:

The data extracted were used to make a scatterplot. A general trend cannot be estimated from scatterplot. For 2017, the PWV fluctuated between 3 mm to 4.8 mm with a peak value of 4.7 mm in May. Similarly, data fluctuated between 4.1 mm to 5.8 mm in June, 5.2 mm to 5.95 mm in August, 4.6 mm to 5.7mm in September, 2.3 mm to 3.85 mm in October, 1.25 mm to 3.2 mm in November, 0.9 mm to 2.7 mm in December of 2017. Moreover, in 2018, PWV fluctuated between 0.85 mm to 1.55 mm in January, 0.55 mm to 2.8 mm in February, 1.1 mm to 3.1 mm in March, 1.0 mm to 3.7 mm in April, 2.5 mm to 4.5 mm in May.

The PWV range lies between 4.1 mm to 5.95 mm in Monsoon, 3 mm to 5.95 mm in Summer, 1.25 mm to 5.7 mm in Autumn, 0.55 mm to 3.2 mm in Winter, 0.55 mm to 3.7 mm in Spring. In the summer and monsoon season, PWV rises to its highest. One reason for this is the increase in heat that increases precipitation. As temperatures rise and the air becomes warmer, more moisture evaporates from land and water into the atmosphere. More moisture in the air generally means we can expect more rain and snow (called precipitation) and more heavy downpours. Similarly, in winter the PWV remains the lowest as the water vapor, and other particles condense into clouds, and the amount of water vapor in the atmosphere decreases.
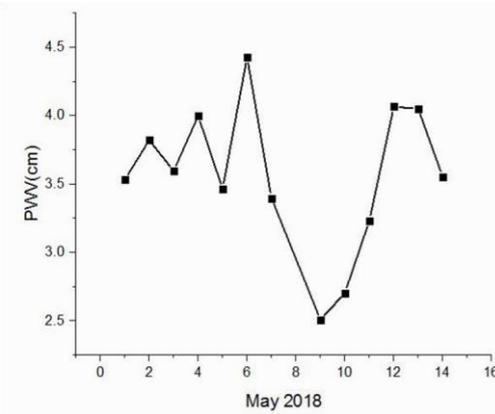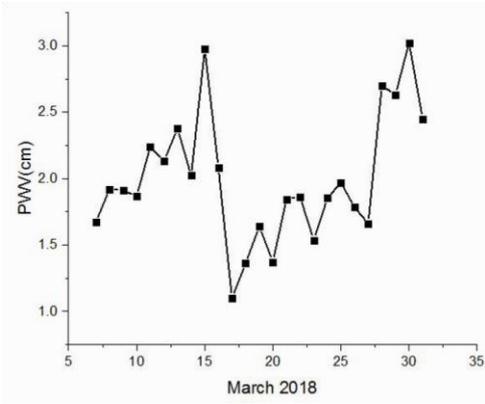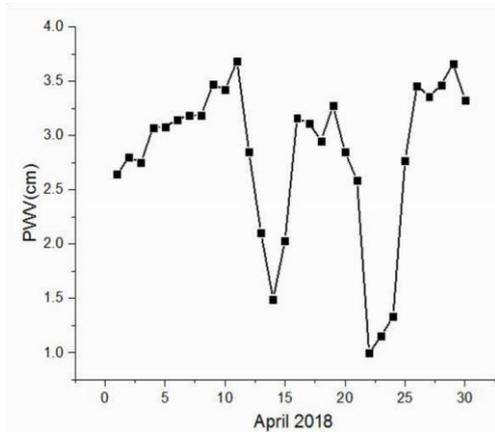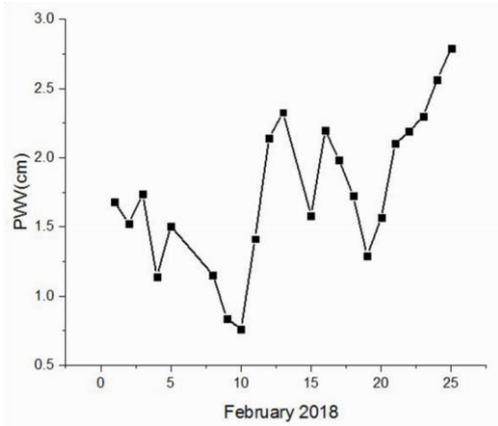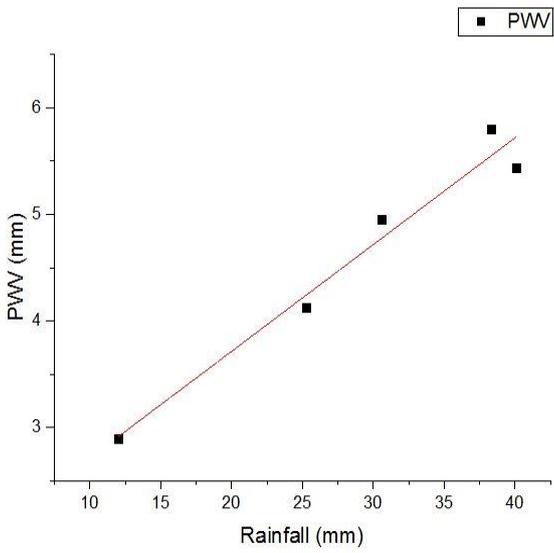
Fig. 2. Graph showing monthly variation of PWV for May 2017 to May 2018

B) Monthly correlation between PWV and rainfall

<.< Fig. 3. Graph showing correlation between PWV and rainfall of the year 2017.
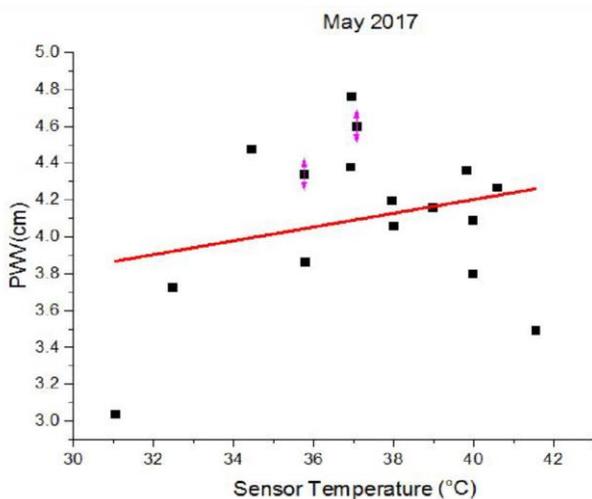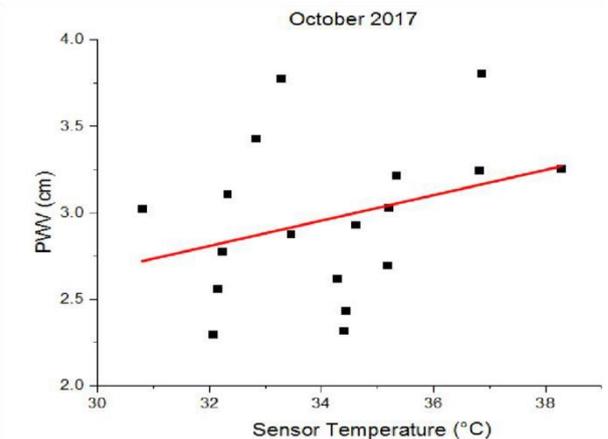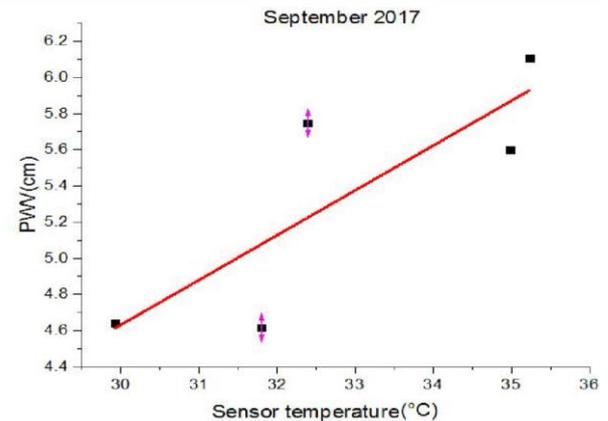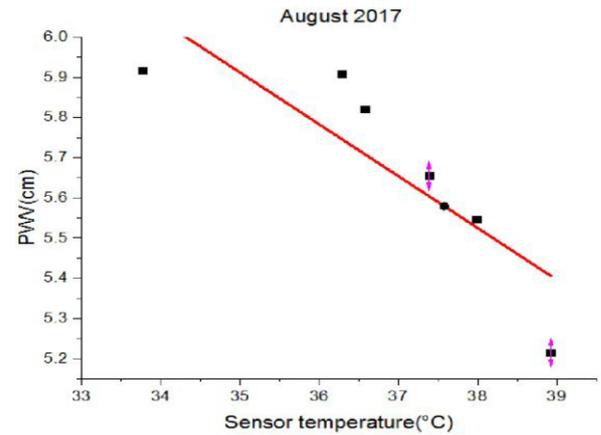
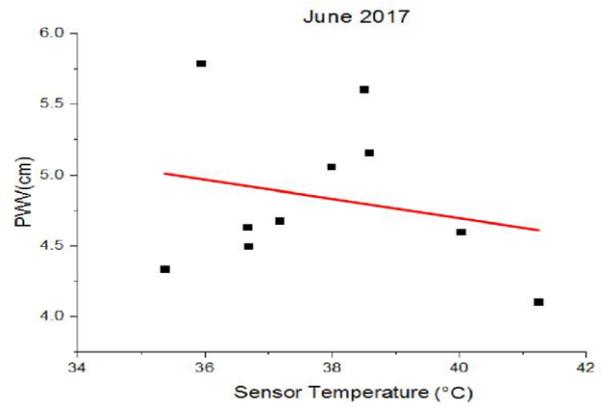We analyzed the trends in precipitable water vapor and rainfall from May 2017 to May 2018, for which both ground-based AERONET and National hydrological data were available. From the given graph we can confirm that precipitable water vapor positively correlates with rainfall. Generally analyzing the trend in rainfall in 2017, it suggest a linear relationship between PWV and rainfall whose equation is given by:

PWV=0.10009*(rainfall(mm))+1.71341   (8)

PWV generally increases before rainfall, and it becomes the highest during rainfall and decreases significantly after the rainfall. According to the data observed, it shows a high correlation of 0.98173 which proves PWV is one of the factors that affect rainfall. Sometimes, there are chances of anomalies, i.e., high precipitable water vapor may not result in rainfall. PWV may be the vital factor for rainfall, but there are external thermodynamic conditions that are necessary to cause rainfall. Despite high PWV, if those external conditions do not meet, rainfall may not occur.

C) Monthly correlation between PWV and sensor temperature

Both of the data of PWV and sensor temperature are recorded with the help of ground-based AERONET. Generally, PWV follows the same trend of sensor temperature as both decreases till December and then increases till May. The lowest precipitable water vapor and the temperature was recorded in January simultaneously. We found negative correlation between PWV and sensor temperature in August, October, and March where precipitable water vapor and temperature has opposite trend. Unusual rainfall pattern could be one reason for the anomalies. For example, In August, although the sensor has decreased, rainfall could cause an increase in precipitation,temperature.
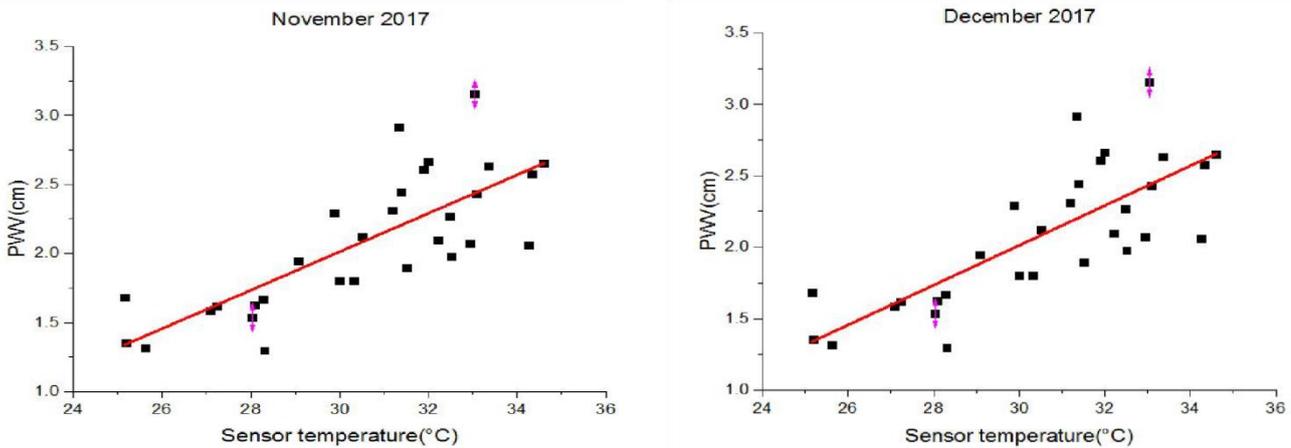
Fig. 4 Monthly plot of PWV against sensor temperature for May 2017 to December 2017

Table II

Slope, intercept, Pearson's(R) and RMSE of PWV and sensor temperature from May 2017 to December 2017

Month/Topics	May	June	August	September	October	November	December
Slope	0.03739 ± 0.03849	-0.06807 ± 0.10244	-0.12899 ± 0.04022	0.24765 ± 0.09902	0.07329 ± 0.0538	0.1392 ± 0.02113	0.05181 ± 0.01853
Intercept	2.70682 ± 1.44088	7.41806 ± 3.87853	10.42675 ± 1.48222	-2.79753 ± 3.26084	0.46392 ± 1.83938	-2.16246 ± 0.64689	0.30592 ± 0.47011
Pearson's coefficient	0.25124	-0.2287	-0.84855	0.82209	0.3224	0.77957	0.50362
RMSE	0.408590349	0.50351	0.13024	0.34397	0.40958	0.30188	0.38865

Due to change in precipitable water vapor, weather pattern and amount of rainfall also get affected. So, why will heavy rainfall occurs as the planet gets warmer? The reason is warmer air holds more water vapor than colder air. Moist air with high precipitation can often cause heavy rainfall. Under favorable conditions, a high amount of precipitable water vapor generally results in higher amount of rainfall and vice versa. Precipitable water vapor is the milestone for meteorologist when following weather pattern. Hence, it becomes one of the vital factors to study climate change and global warming.

The trend in precipitable water vapor is expected to increase the frequency of extremely high rainfall and weather change. The consequences of heavy rainfall would be increased flash flooding and riverine flooding. In the future, by studying the trend in PWV the climatic change could be estimated and retrofitting of climate can be done with techniques such as flood mitigation, and managing urban water flows.

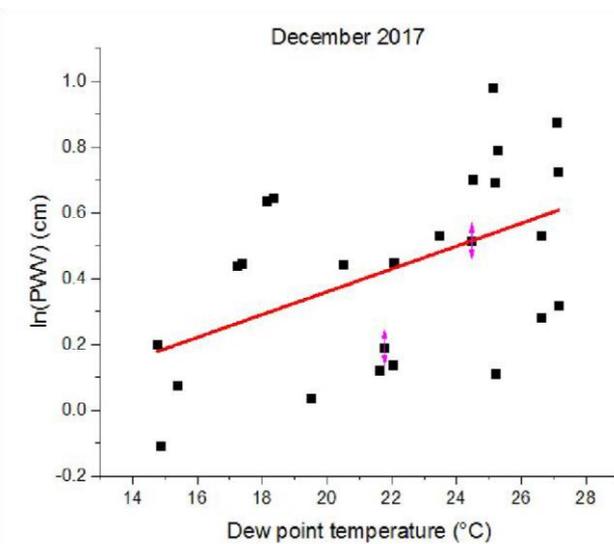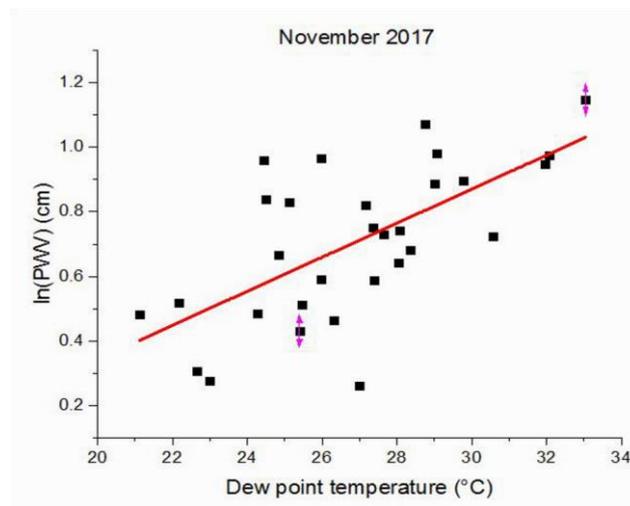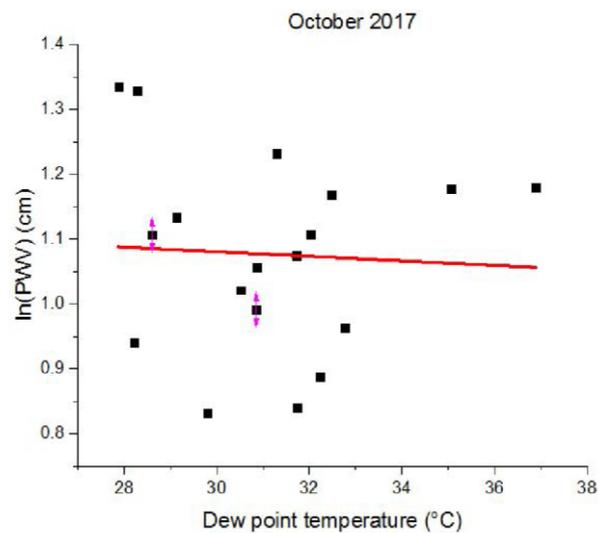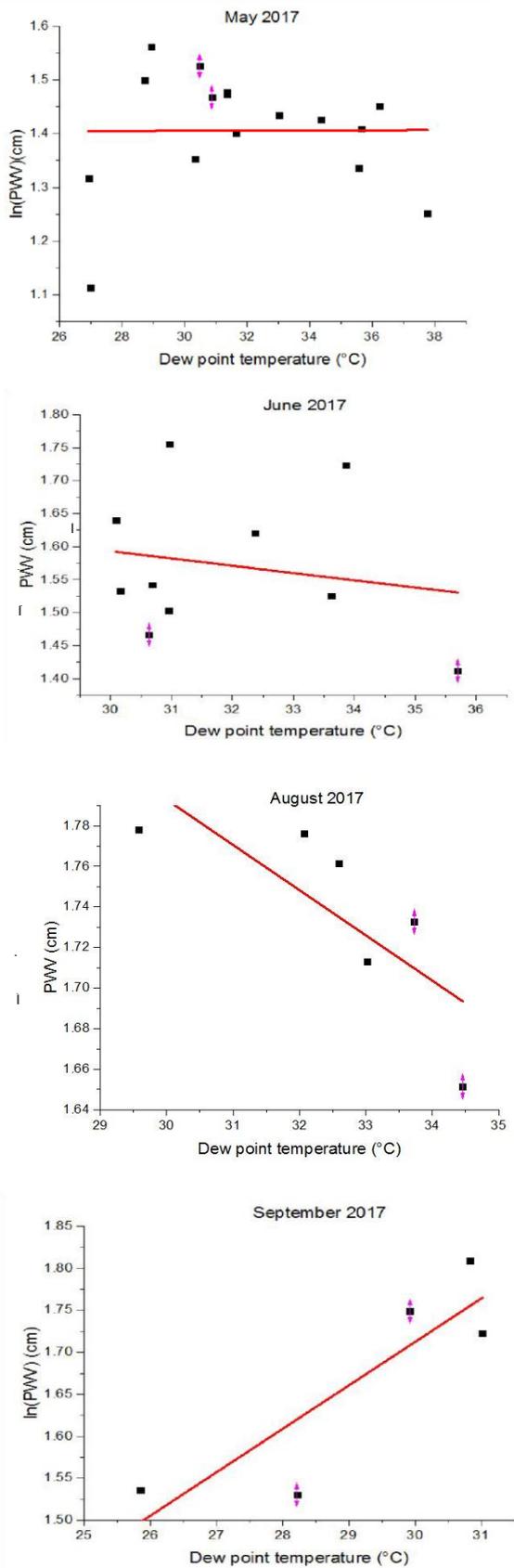D) *Monthly correlation between PMV and dew point temperature*

Fig. 5. Monthly plot of PWV against dew point temperature for May 2017 to December 2017

Table III
slope, intercept, Pearson's(R) and RMSE of PWV and dew point temperature from May 2017 to December 2017

Month/Topics	May	June	August	September	October	November	December
Slope	1.74414E-4 ± 0.00915	-0.01099 ± 0.02014	-0.02228 ± 0.00895	0.05174 ± 0.01686	-0.0035 ± 0.01576	0.0527 ± 0.01173	0.03464 ± 0.01265
Intercept	1.40025 ± 0.29341	1.92266 ± 0.64357	2.4613 ± 0.29185	0.16008 ± 0.49296	1.18538 ± 0.49197	-0.71085 ± 0.31722	-0.33279 ± 0.2835
Pearson's coefficient	0.00509	-0.1894	-0.7796	0.87081	-0.05536	0.64712	0.49592
RMSE	0.10896	0.10291	0.02767	0.0565	0.14538	0.17988	0.24398

Generally, distribution on the figure is linear and slope and intercept for the graph is given in table and equation is given by:

$$\ln(PWV) = k_1 T_d + k_2 \qquad (9)$$

Where, k_1 = slope which varies from (-0.02228 to 0.05174)
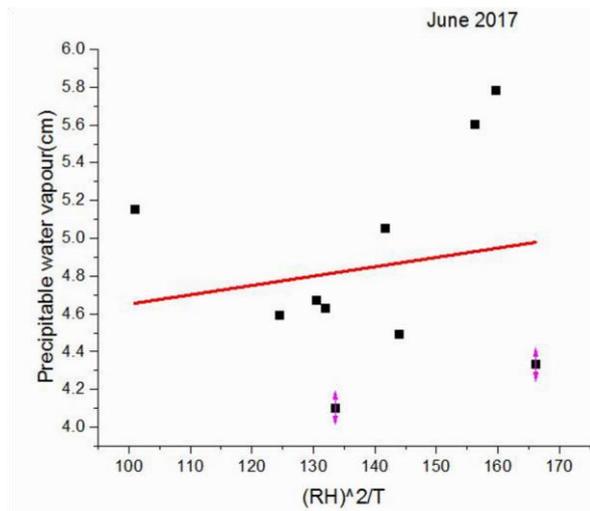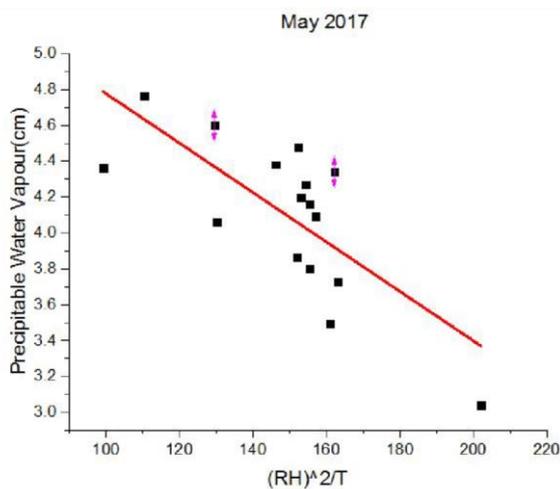
k_2 = intercept of graph which varies from (-0.71085 to 2.4613)-

Maximum Pearson's R was found in month of September with a value of 0.87081 and minimum was found in month of May with a value of 0.00509. The maximum and minimum RMSE was found in month of December and August with values of 0.24398 and 0.02767 respectively. Most of the months show good coefficient of correlation. The error in the values could be due to lack of enough availability of data. Slope of PWV (T) could be used as an indicator of the moisture burden of a place, that is, the more the slope value the less water vapor mixing ratio

As we can see that August has lowest value of slope i.e. hence, it has higher water vapor mixing ratio hence, August is wetter than other months. Similarly, November has the highest value of slope which refers that it has lowest water vapor mixing ratio and hence, it is one of the driest season of the year. As season changes from summer to winter slope gradually increases and hence season becomes drier as it approaches winter season. In summer, the heat causes cloud to vaporize and increases water vapor mixing ratio in environment and vice versa.

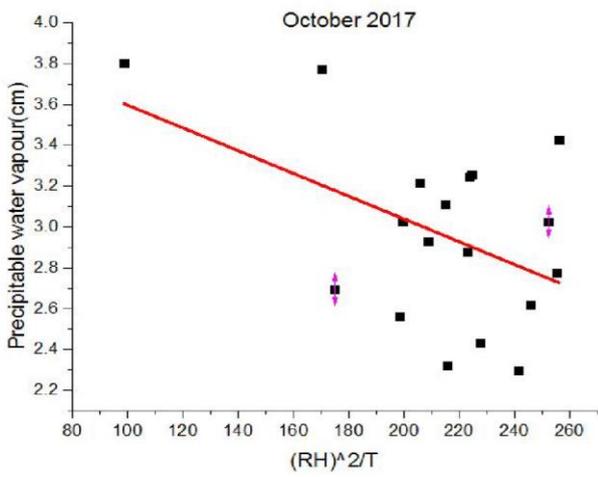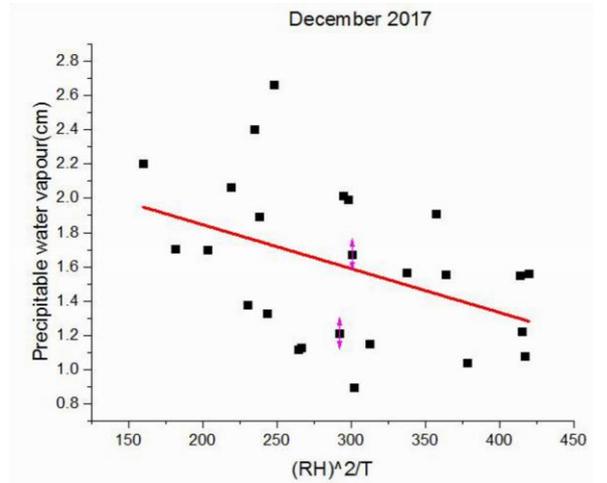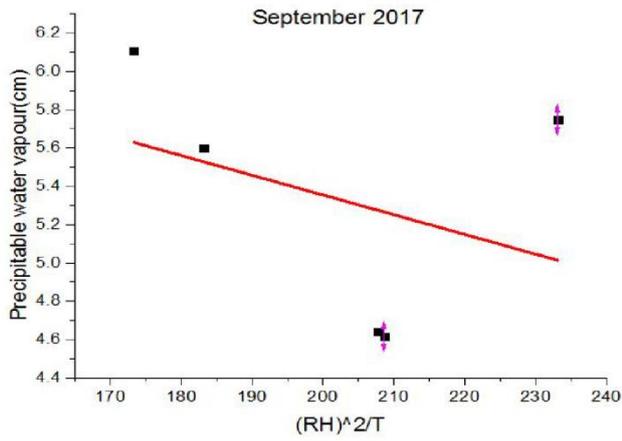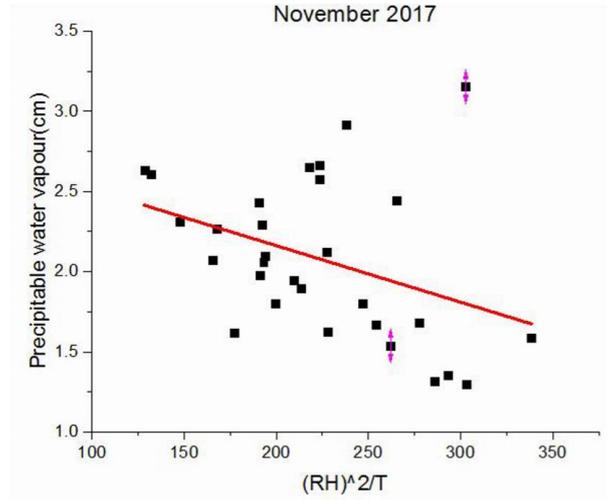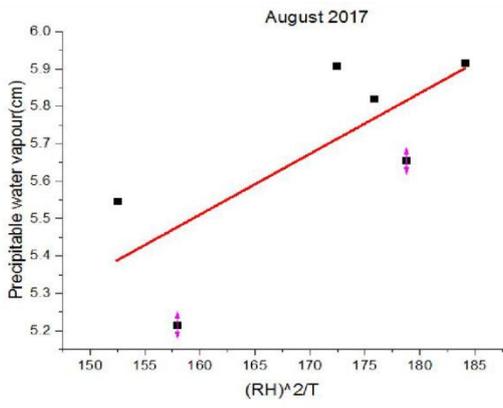*E) Monthly correlation of relative humidity and PWV*

Fig. 6. Plot of square of relative humidity divided by temperature against PWV for May 2017 to December 2017

Table IV
slope, intercept, Pearson's(R), and RMSE of $(RH)^2/T$ and PWVfor May 2017 to December 2017

Month/Topics	May	June	August	September	October	November	December
Slope	-0.01378 ± 0.00333	0.00495 ± 0.00991	0.01625 ± 0.00723	-0.01028 ± 0.01546	-0.00557 ± 0.00258	-0.00352 ± 0.00163	-0.00256 ± 0.00113
Intercept	6.15499 ± 0.5023	4.15656 ± 1.38736	2.91106 ± 1.23298	7.41099 ± 3.12678	4.15262 ± 0.55825	2.86709 ± 0.37356	2.35757 ± 0.3458
Pearson's coefficient	-0.74141	0.17389	0.74719	-0.35851	-0.47472	-0.37771	-0.42603
RMSE	0.28327	0.50933	0.16359	0.16359	0.38082	0.446287	0.407

Relative humidity (RH) is a measure of atmospheric moisture and a basic meteorological Parameter. Hence an attempt was made to develop empirical relation between the PWV and Relative humidity square by temperature $(RH)^2/T$. The relation was linear and the graphs suggested the equation i.e.

$$PWV = \frac{k_1(RH)^2}{T} + k_2 \qquad (10)$$

Where,

k_1 is the slope of the equation and varies from -0.00557 to 0.01625 and

k_2 is the intercept which varies from 2.35757 to 6.15499

The good correlation between the PWV and relative humidity is not unexpected since relative humidity is also a measure of atmospheric moisture content. However, the dew point temperature being a more direct measure of atmospheric moisture content than the relative humidity, generally show a better correlation with the PWV than the relative humidity does with PWV. For most of the months, Pearson's R of dew point temperature is more than that of $(RH)^2/T$. For example, It is known that a relationship exists between some measure of the water vapor content of the air near the surface and the amount of moisture aloft. If the moisture content of the air at any upper level is related to the amount of moisture at the surface, then it follows that the total water vapor content of the air would also be related to a measure of surface moisture. Precipitable water can be used as a good indicator of total moisture. A fairly good relationship has been reported in the literature between surface moisture parameters like relative humidity with precipitable water vapor.

The maximum and minimum correlation between PWV and $(RH)^2/T$ was 0.74719 and 0.17389 in the month of August and June respectively. Moreover there exists negative correlation in the months of May, September, October, November and December. The maximum and minimum RMSE was found to Be 0.50933and 0.16359 in the months of June and August respectively.
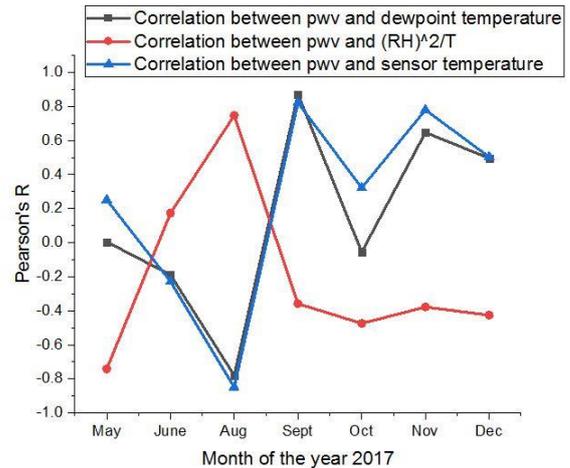

Fig. 7. Combined correlation graphs for the year 2017.

V. CONCLUSION

Using monthly averaged surface meteorological data obtained from AERONET for station across Lumbini for May 2017- May 2018, correlation between PWV, dew point temperature,sensor temperature, and relative humidity were obtained. Generally the months in which the error in the slope is minimum, those months shows maximum correlation and act as a better predictor for the relation.. Moreover, dew point temperature and sensor temperature follow a

similar correlation pattern with PWV. Correlation pattern for $(RH)^2/T$ and PWV is opposite in nature till September and then follows similar trend as dew point temperature and sensor temperature till December. Generally, August has low amount of data as most of the days in August are cloudy. Hence, it could be one of the reasons for the opposite pattern in correlation. It has shown good correlation coefficient between them with highest correlation existing between PWV and Rainfall. Correlation between PWV and dew point temperature was generally higher than PWV and relative humidity per degree centigrade. The data of 2017 to 2018 have been used to evaluate several empirical expressions based on conventional moisture measurements available in this region (i.e. relative humidity, sensor temperature and dew point temperature). These empirical formulas have low amount of RMSE and hence they are good predictor of precipitable water vapor in Lumbini region. Anomalies in research could be due to lack of analysis of enough amount of data. Due to critical importance of PWV in climate research, it is of great interest to correctly estimate moisture parameters in climate models.

VII. REFERENCES

[1] Barreto, A., Cuevas, E., Damiri, B., Romero, P. M., & Almansa, F. (2013). Column water vapor determination in night period with a lunar photometer prototype. *Atmospheric Measurement Techniques*, *6*(8), 2159–2167. https://doi.org/10.5194/amt-6-2159-2013

[2] Bruegge, C.J., Conel, J.E., Green, J.S., Margolis, J.S., Holm, R.G., Toon, G., 1992. Water vapor column abundance retrievals during FIFE. J. Geophys. Res. 97, 759e768.

[3] Chance, K. (2006). Remote Sensing of the Atmosphere for Environmental Security. *Remote Sensing of the Atmosphere for Environmental Security*, (February), 1–25. https://doi.org/10.1007/978-1-40205090-9

[4] Falaiye, O. A., Abimbola, O. J., Pinker, R. T., Pérez-Ramírez, D., & Willoughby, A. A. (2018). Multitechnique analysis of precipitable water vapor estimates in the sub-Sahel West Africa. *Heliyon*, *4*(9). https://doi.org/10.1016/j.heliyon.2018.e00765

[5] Holben, B.N., Eck, T.F., Slutsker, I., Tanre, D., Buis, J.P., Setzer, A., Vermote, E., Reagan, J.A., Kaufman, Y.A., 1998. AERONET-a federated instrument network and data achieve for aerosol characterization. Remote Sens. Environ. 66, 1e16.

[6] Li, J., Lv, Q., Zhang, M., Wang, T., Kawamoto, K., Chen, S., & Zhang, B. (2017). Effects of atmospheric dynamics and aerosols on the fraction of supercooled water clouds. *Atmospheric Chemistry and Physics*, *17*(3), 1847–1863. https://doi.org/10.5194/acp-17-1847-2017

[7] Mears, C. A., Santer, B. D., Wentz, F. J., Taylor, K. E., & Wehner, M. F. (2007). The relationship between temperature and precipitable water changes over tropical oceans. *Geophysical Research Letters*, *34*(24), 1–5. https://doi.org/10.1029/2007GL031936

[8] Mishra, M. R., Behera, R. K., Jha, S., Panda, A. K., Mishra, A., Pradhan, D. K., & Choudary, P. R. (2011). A brief review on phytoconstituents and ethnopharmacology of Scoparia dulcis Linn. (Scrophulariaceae). *International Journal of Phytomedicine*, *3*(4), 422–438. https://doi.org/10.1002/qj

[9] Reagan, J.A., Thome, K., Herman, B., Gall, R., 1987. Water vapor measurements in the 0.94 micron absorption band: calibration, measurements and data applications. In: Proc. Int. Geosci. Remote Sens. Symp., pp. 63e67. IEEE 87CH2434-9.

[10] Smirnov, A., B. N. Holben, A. Lyapustin, I. Slutsker, and T. F. Eck (2004), AERONET processing algorithms refinement: Proceedings of AERONET workshop, El Arenosillo, Spain, NASA/GSFC Aeronet project.

[11] Torres, B., Cachorro, V. E., Toledano, C., Galisteo, J. P. O. De, Berjón, A., Frutos, A. M. De, … Laulainen, N. (2010). Precipitable water vapor characterization in the Gulf of Cadiz region (southwestern Spain) based on Sun photometer , GPS , and radiosonde data, 115, 1–11. https://doi.org/10.1029/2009JD012724

[12] Varamesh, S., Hosseini, S. M., & Rahimzadegan, M. (2017). Estimation of atmospheric water vapor using MODIS data 1. (case study: Golestan province of Iran). *Journal of Materials and Environmental Science*, *8*(5), 1690–1695.

[13]   Wang, Y., Tang, L., Zhang, J., Gao, T., Wang, Q., Song, Y., & Hua, D. (2018). Investigation of precipitable water vapor obtained by Raman lidar and comprehensive analyses with meteorological parameters in Xi'an. *Remote Sensing*, *10*(6), 1–16. https://doi.org/10.3390/rs10060967

[14]   Westwater, Ed & Cimini, D & Mattioli, Vinia & Gasiewski, Al & Klein, M & Leuski, Vladimir & Liljegren, James. (2006). The 2004 North Slope Of Alaska Arctic Winter Radiometric Experiment: Overview and Highlights. 77 - 81. 10.1109/MICRAD.2006.1677066.

[15]   Yao, Y., Shan, L., & Zhao, Q. (2017). Establishing a method of short-term rainfall forecasting based on GNSS-derived PWV and its application. *Scientific Reports*, *7*(1), 1–11. https://doi.org/10.1038/s41598-017-12593-z